Composites Communications **43 (2023) 101723**

https://doi.org/10.1016/j.coco.2023.101723

A bistable helical structure based on composite tape-springs

Biao Xu[1,2], Bing Wang[1,2*], Kevin S Fancey[3], Shuncong Zhong[1,2], Chenmin Zhao[1,2], Xiayu Chen[1,2]

[1] Fujian Provincial Key Laboratory of Terahertz Functional Devices and Intelligent Sensing, School of Mechanical Engineering and Automation, Fuzhou University, Fuzhou, 350108, P.R. China

[2] Institute of Precision Instrument and Intelligent Measurement & Control, Fuzhou University, Fuzhou 350108, P.R. China

[3] School of Engineering, University of Hull, Hull HU6 7RX, United Kingdom

[*] Corresponding to: b.wang@fzu.edu.cn (B. Wang)

Abstract: Conventional twistable structures use discrete parts articulated around a number of linkages. These allow only a limited degree of twisting angle, are low in storage ratio, heavy and complex in morphing mechanisms. Double-helix structures are commonly applied to induce twistable shape-changing capability for deployable structures, these being capable of large axial deformations where prestressed thin-shell composite flanges or strips are employed; however, their structural stabilities are susceptible to thermal effects, and suffer from non-zero Gaussian curvature deformation induced by prestressing of the precured flat strips. Here, we propose a novel bistable helical structure, where zero Gaussian curvature deformation applies, and shows more stable and reliable morphing mechanics for a twistable structure to be engineered. This is achieved by exploiting bistable composite tape-spring (CTS) structures, where two CTS samples are pin-joined through spokes to formulate a helical structure. It is capable of large axial morphing, and stable in both the fully extended and twisted configurations, with adjustable storage ratio. A theoretical model was established to predict its bistability and a bespoke axial displacement rig was developed to investigate its non-linear morphing mechanisms in order to reveal the underlying fundamentals. These will facilitate torsional structural design for aerospace deployable structures.

Keywords: Bistable; Helical structure; Composite; Tape-spring.

1 Introduction

Advanced composite materials have been widely used in mechanical engineering applications, especially in the fields of aerospace, medical and renewable energy, due to their superior properties in terms of specific strength and modulus, design flexibility, and corrosion resistance, etc. [1]. Specifically, bistable or multistable structures can be designed and manufactured by using composites which are stable in at least two configurations, and endure repeated shape-changing processes when subjected to external stimuli [2]. There is growing interest in their applications to aerospace deployable structures [3], energy harvesting systems [4], soft actuators and robots [5], as well as advanced functional devices [6].

Bistable composite structures can be produced by adjusting in-plane stress levels [7]; these have been reported to be achieved by means of thermal residual stresses [8,9], piezoelectric actuator [10], elastic fibre prestressing [11,12], viscoelastic fibre prestressing [13,14], prestressing cured composite laminate [15], as well as geometric curvature effects [16,17]. In particular, a bistable structure produced by adopting geometric curvature effects is known as a bistable composite tape-spring (CTS), which is derived from the carpenter’s tape principle [18]: it is stable in both extended and coiled configurations with fibres oriented at ±45° [19]. Although bistable composite technologies have been a proven technique, only CTS-based morphing structures have been applied in aerospace industries: a CTS-based roll-out solar array was launched to the International Space Station in November 2017 [20], and subsequently applied on a Double Asteroid Redirection Test satellite in September 2022 [21].

There are growing attempts to reduce weight and complexity for twistable structures in aerospace, where composites have also drawn great expectations. Conventional twistable shape-changing structures use discrete parts articulated around a number of linkages; they allow only a limited degree of torsional angle, are low in storage ratio, heavy and have complex shape-changing mechanisms. A double-helix composite structure is applied to induce twisting deployable capability, which is capable of large axial shape-changing. Lachenal et al. [22] used two prestressed precured composite flanges joined together to form a double-helix structure, which showed zero stiffness along the twisting axis. Since the I-beam is in a high state of elastic strain energy, the initial stable shape is in a twisted configuration, and suffer from non-uniform deformation induced by unsymmetric prestressing of the precured strips [23]. Subsequently, it is further demonstrated that the stability of the helical structure depends on the geometric boundaries and non-zero Gaussian curvature effects, indicating an equally un-symmetric force/displacement characteristic of the helix [24]. Thermal effects on the stability of the bistable composite helices showed that they could enhance the viability of multi-stable composite helical structure [25]. A refined model was then developed by considering both transverse curvature and membrane strains, associated with non-zero Gaussian curvature deformation, leading to a complex interplay between membrane and bending strain energies [26]. The strain energy is stored by prestressing precured composite strips, and then connected to spokes, which leading to non-uniform and nonlinear distribution of strain energy. Aza et al. [27] developed a truss-like compliant mechanism to analyse the factors that affecting twisting deformation along the length of the helical structure. Their findings indicated that composite layups, friction between spokes and prestressed strips, imperfections during manufacturing, as well as the length-to-radius ratio of the helices were all contributions to the non-uniform twisting process.

Therefore, composite-based twistable morphing structures are mainly focused on using prestressed composite flanges or strips to construct the helical structures; however, they are susceptible to thermal effects [25], and suffer from non-zero Gaussian curvature [24]. Here, we propose a novel bistable helical structure with zero Gaussian curvature, which shows more stable and reliable morphing mechanics for a twistable structure to be engineered. This is achieved by exploiting bistable CTS structures, where two CTS samples are pin-joined through spokes to formulate a helical structure, which is capable of large axial shape-changing, and stable in both the fully extended and twisted configurations. A theoretical model based on the zero Gaussian curvature deformation induced inextensional strain energy principle was established by considering the helical geometry and composite orthotropy, in order to predict its bistability and corresponding strain energy path of the shape-changing process; a bespoke axial displacement rig was then developed to investigate its non-linear morphing mechanisms in order to reveal the underlying fundamentals.

2 Theoretical analysis

2.1 Structural constitutive

A CTS structure is an open-slit tube with fibres oriented at ±45°. Its structural parameters include tape length, thickness, initial radius, and subtended angle, denoted as L, t, R, and β, respectively. Figure 1 schematically shows typical structural configurations of a CTS-based bistable helical structure, associated with its axial shape-changing under axial displacement or twisting moment in terms of both the twisted angle, defined as $\varphi = L\sin\theta/r$, and the axial displacement per unit length, $\delta = 1 - \cos\theta$, as a function of the helical angle, $\theta\,(-\pi/2 \le \theta \le \pi/2)$. The CTS-based helical structure is composed of two CTS samples, pin-jointed together with rigid spokes, where torsional freedom is released in order to be twistable. Figure 1 (a) presents the structural definition of the representative volume unit (RVU), where, a is the unit length, and the helical structure technically has infinite numbers of RVU, i.e. the length is theoretically $n \times a$. The length and diameter of the spokes are represented by $2r$ and d_0. Figure 1 (b) gives the extended stable configuration, Fig. 1 (c) is an intermediate twisted shape, and Fig. 1 (d) is the fully-twisted stable configuration.

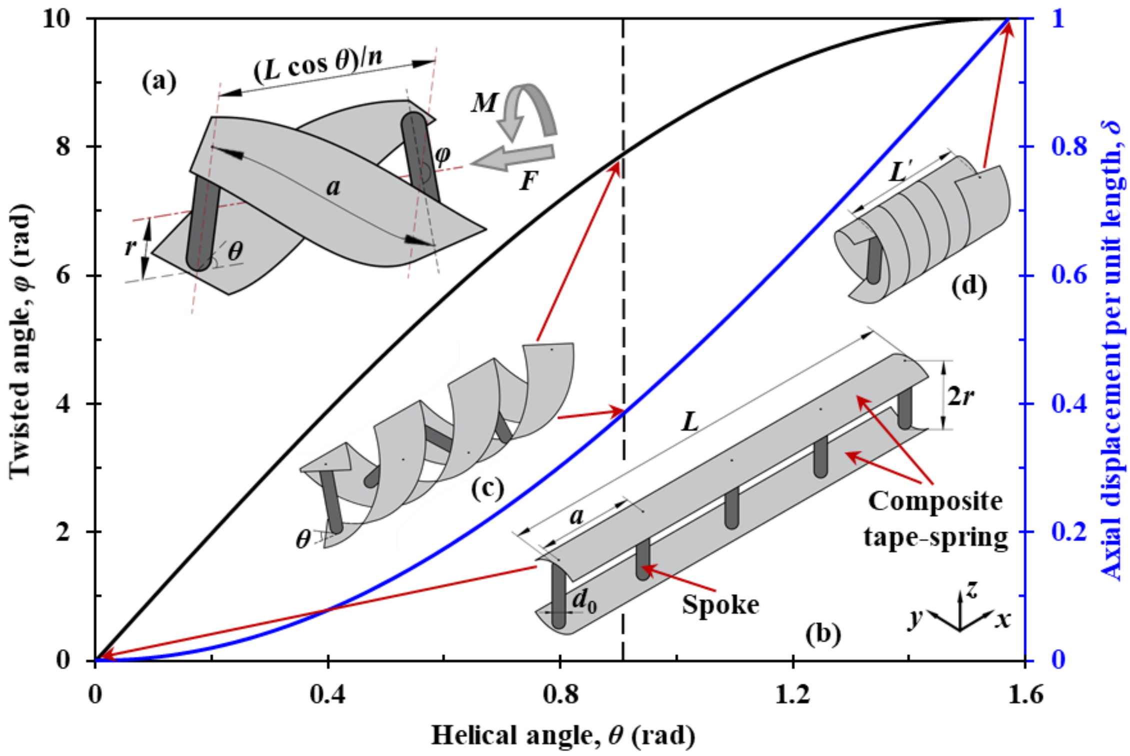

Fig. 1 **Schematic diagram of a bistable helical structure based on composite tape-springs, showing the axial shape-changing process in terms of both the twisted angle, *φ*, and the axial displacement per unit length, *δ*, as a function of the helical angle, *θ*; insets present: (a) the constitutive definition of the representative volume unit; (b) extended stable configuration; (c) intermediate twisted shape; (d) fully-twisted stable configuration.**

2.2 Structural bistability

Bistability of a CTS is a well-known concept; it is governed by material constitutive behaviour, initial geometrical proportions, and geometrically non-linear structural behaviour. Assuming the shape-changing process of the helical structure is inextensional and uniform, the Gaussian curvature remain zero [17]. The inextension assumption indicates that the bending strain energy of thin shells dominates the strain energy associated with stretching [22,23]. Assuming there is no friction between spokes and CTS, effects from pin-jointed holes on structural strain energy are marginal, the strain energy, U, of the CTS-based bistable helical structure is:

$$U = \boldsymbol{\Delta\kappa}^{\mathrm{T}}\mathbf{D}^{*}\boldsymbol{\Delta\kappa}L\beta R \tag{1}$$

where, $\boldsymbol{D}^{*} = \boldsymbol{D} - \boldsymbol{B}\boldsymbol{A}^{-1}\boldsymbol{B}$ is the reduced bending stiffness matrix of the composite tape with $\boldsymbol{A}$, $\boldsymbol{B}$, and $\boldsymbol{D}$ are the in-plane, bending-extension coupling and flexural stiffness matrices, respectively, whilst for our plain-weave composite tape with symmetric layup, $\boldsymbol{B} = 0$; a structural ratio, α, is defined as the value of the initial radius R of the CTS to the fully-twisted radius r of the helical structure. The change in curvature to any configuration of a CTS can be described by a tensor $\boldsymbol{\Delta\kappa}$:

$$\boldsymbol{\Delta\kappa} = \begin{bmatrix} \Delta\kappa_x \\ \Delta\kappa_y \\ \Delta\kappa_{xy} \end{bmatrix} = \frac{1}{2r}\begin{bmatrix} 1-\cos(2\theta) \\ 1+\cos(2\theta)-2/\alpha \\ 2\sin(2\theta) \end{bmatrix} \tag{2}$$

where, $\Delta\kappa x$, $\Delta\kappa y$, and $\Delta\kappa xy$, are the curvature changes in longitudinal, transverse and twisting directions, respectively. Eqn (1) is now:

$$U = \frac{L\beta R}{4r^2}\left(D_{11}^*\left(1-\cos(2\theta)\right)^2 + 2D_{12}^*(1-\cos(2\theta))\left(1+\cos(2\theta)-\frac{2}{\alpha}\right) + D_{22}^*\left(1+\cos(2\theta)-\frac{2}{\alpha}\right)^2 + 4D_{66}^*\sin^2(2\theta)\right) \tag{3}$$

The stable equilibrium positions of the bistable helical structure could be obtained by minimising the Eqn (3) with respect to two variables, θ and α. It is worth noting that the ratio α is a constant value for any bistable helical structure. Thus, the helical angle θ is the only independent variable of the strain energy U. Consequently, the equilibrium position of the structure is determined when the first derivative of U with respect to θ is equal to zero and the second derivative is strictly positive:

$$\frac{\partial U}{\partial \theta} = \frac{L\beta R}{r^2}\left(D_{11}^*\sin(2\theta)\left(1-\cos(2\theta)\right) + 2D_{12}^*\sin(2\theta)\left(\cos(2\theta)-\frac{1}{\alpha}\right) + D_{22}^*\sin(2\theta)\left(\frac{2}{\alpha}-1-\cos(2\theta)\right) + 2D_{66}^*\sin(4\theta)\right) = 0 \tag{4}$$

$$\frac{\partial^2 U}{\partial \theta^2} = \frac{2L\beta R}{r^2}\left(D_{11}^*\left(\cos(2\theta)-\cos(4\theta)\right) + 2D_{12}^*\left(\cos(4\theta)-\frac{\cos(2\theta)}{\alpha}\right) + D_{22}^*\left(\left(\frac{2}{\alpha}-1\right)\cos(2\theta)-\cos(4\theta)\right) + 4D_{66}^*\cos(4\theta)\right) > 0 \tag{5}$$

3 Experimental

Table 1 shows the material properties of the plain-weave carbon prepreg used in this research, which was supplied by Kabenfanbo Composites Co., Ltd., China. To produce a bistable helical structure with three RVUs, two CTS samples and four rigid radial spokes with the same geometrical configuration were used. First, carbon prepreg was cut into specific sizes with fibres oriented at ± 45°. The prepared layup was placed between two PTFE coated glass fabric papers, and then gradually wrapped and tightened around a cylindrical mandrel by using a heat shrinkage tape. The mould was then subjected to heat treatment under 120 °C for 120 minutes using a fan-assisted oven. Finally, the CTS samples were pin-jointed with the spokes to produce a bistable helical structure. The CTS was typically 250 mm in length, 12.5 mm in initial radius, 0.18 mm in thickness and subtended 114°; the spokes were 50 mm in length, with a diameter of 10 mm, and a radius of 5 mm at both ends.

Table 1 Materials properties of the plain-weave carbon prepreg.

Type	Specification	
Fabric	Fibre	Carbon T300-3k
	Woven	Plain-weave
	Fibre area weight	200 g/m^2
Prepreg	Thermoset resin	Epoxy WP-R5600W3K
	Gel time	~798 s @ 120°C
	Fibre volume fraction	42%
Laminate	0° Elastic modulus	57 GPa
	0° Tensile strength	740 MPa
	Shear modulus, G_{12}	3.5 GPa
	Poission's ratio, ν	0.075
	0° Compressive strength	670 MPa
	0° Flexural strength	860 MPa

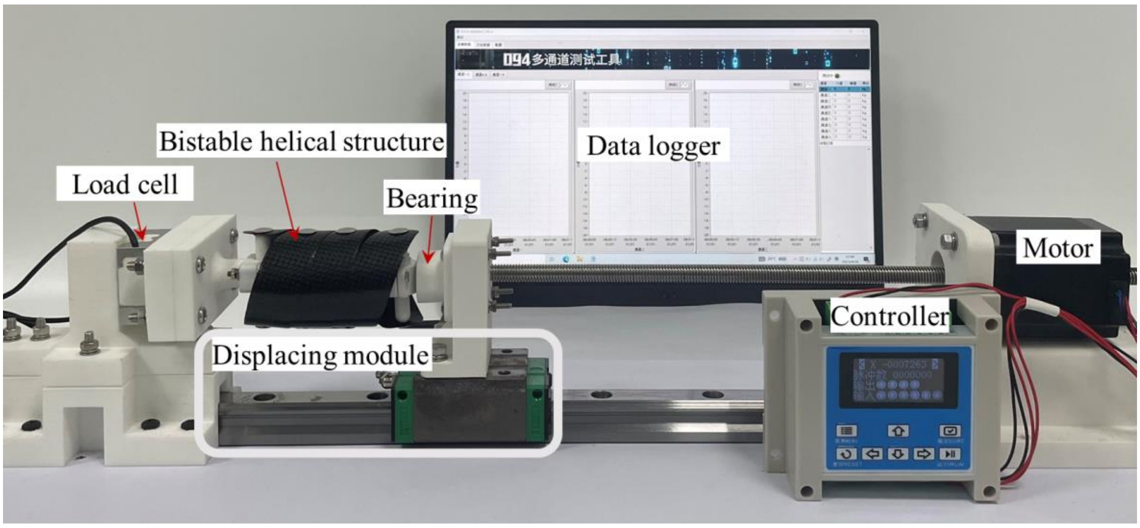

Fig. 2 Experimental setup of the bespoke axial displacement rig used to monitor the shape-changing process of the bistable helical structure.

A bespoke axial displacement rig was developed to characterise the non-linear shape-changing process of the bistable helical structure. Figure 2 shows the experimental setup: the spoke at the left end of the helical structure was clamped centrally to a load cell and the right end spoke was connected to a bearing to twist freely. A displacing module was employed to apply axial displacement at a constant speed of 60 mm/min. The bistable helical structure was tested three times for repeatability; axial reaction load was monitored for both the loading and unloading processes.

4 Results and discussion

Figure 3 (a) shows a polar plot of the helical structural strain energy U calculated by using Eqn (3) as a function of the structural ratio, α, and helical angle, θ. For the fabricated bistable helical structure, α is found to be 0.5: although the real structural strain energy does not fall within the local minimum points as demonstrated by the red dots, it still exhibits bistability. Thus, the strain energy path along the contour line when $\alpha = 0.5$ is further demonstrated in Fig. 3 (b), associated with typical shapes from a real bistable helical sample. Although the fabricated bistable helical structure is not essentially "stress free", it is clear that it is stable in both the extended and fully-twisted configurations as denoted by points A and C. Point B is a saddle point, where snap occurs when subjected to axial displacement. This is further characterised through experimental tests below.

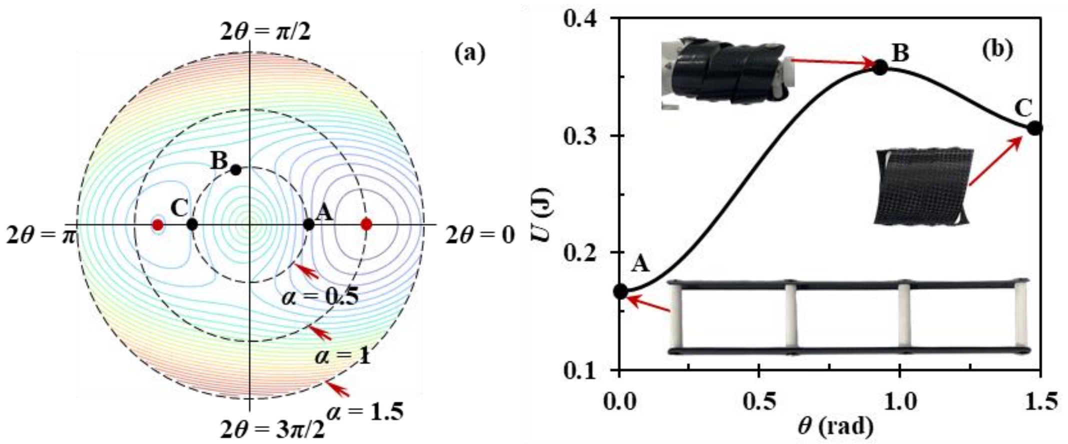

Fig. 3 **(a) A polar plot of the helical structural strain energy *U* calculated by using Eqn (3) as a function of the structural ratio, α, and helical angle, θ; (b) the strain energy path along the contour line when $\alpha = 0.5$, associated with typical shapes from a real bistable helical structure.**

Figure 4 shows the experimental characterisation of the non-linear shape-changing process of the bistable helical structure when subjected to axial displacement. Both the loading and unloading processes are presented, together with typical non-uniform twisted sample shapes. It is clear that when subjected to axial displacement, the load increases linearly until it reaches the local maximum value in order to initiate twist of the helical structure: this is attributed to the bending-twisting coupling as previously observed on three-point bending of a CTS structure [18]. The structure then starts to undergo twisted deformation with stablised load, as demonstrated by the insets. When displaced to around 60 mm, there are clear axial offsets around the centre of the helix resulting from local shear buckling, which recovers quickly. The saddle shape presented by point B in Fig. 3 corresponds to a displacement of 175 mm, giving a local snapping peak. On approaching the fully-twisted configuration, the load increases nonlinearly; this may be attributed to local impact after snapping, as well as manufacturing imperfections, which lead to early contact between the tapes and spokes. The unloading process is relatively stable without local shear buckling, whilst there is a local minimum peak which may be generated by friction between the tapes and spokes. This results in a non-uniform distribution of helical angles along the two tapes in the axial direction as highlighted by the insets in Figure 4.

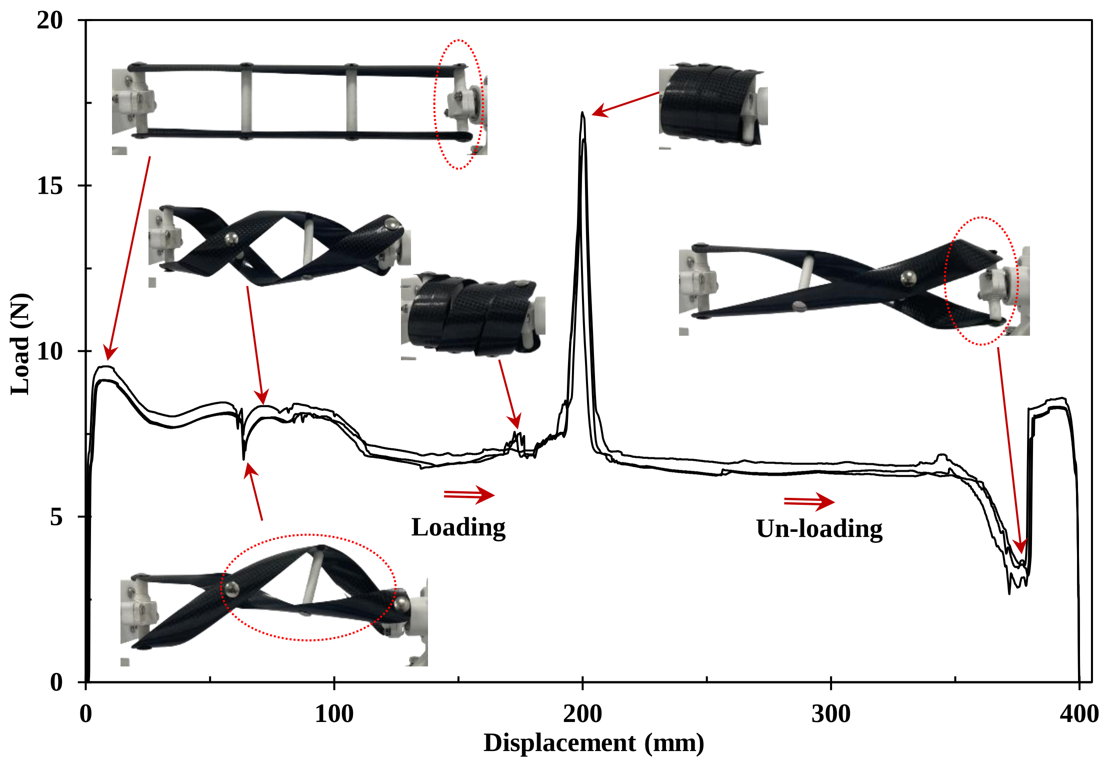

Fig. 4 **Experimental characterisation of the non-linear shape-changing process of the bistable helical structure when subjected to axial displacement. Both the loading and unloading processes are presented, together with typical non-uniform twisted sample shapes.**

5 Conclusions

We have devised a novel composite tape-spring-based bistable helical structure, which is stable in both the extended and fully-twisted configurations, and is capable of repeated large axial morphing with an adjustable storage ratio. The bistable helical structure was produced with zero Gaussian curvature, where two CTS structures were pin-jointed through spokes. A theoretical model based on the zero Gaussian curvature deformation induced inextensional strain energy model was consequently established by considering the real helical geometry and composite orthotropy, and agreed well with experimental observations. It infers that although the fabricated bistable helicalstructure is not essentially "stress free", the positive difference in strain energy between the onset of snap (from axial twisting) to the fully twisted configuration indicates bistability. A bespoke axial displacement rig was then developed to investigate the shape-changing mechanisms of the helical structure. It is found that when subjected to axial displacement, the bistable helical structure will experience bending-twisting coupling, local shear buckling, as well as snapping which is generated by its bistable nature. These will facilitate torsional structural design for aerospace deployable structures. Work is currently on-going in order to reveal further on the geometric constraints and morphing mechanics of the bistable helical structure.

CRediT authorship contribution statement

Biao Xu: Investigation, Data curation, Software, Formal analysis, Writing – original draft. **Bing Wang:** Investigation, Supervision, Formal analysis, Writing – original draft, Writing – review & editing, Funding acquisition. **Kevin S. Fancey:** Validation, Writing – review & editing. **Shuncong Zhong:** Supervision, Writing – review & editing, Funding acquisition. **Chenmin Zhao:** Validation, Writing – review & editing. **Xiayu Chen:** Validation, Writing – review & editing.

Declaration of competing interest

The authors declare that they have no known competing financial interests or personal relationships that could have appeared to influence the work reported in this paper.

Data availability

Data will be made available on request.

Acknowledgements

The authors are grateful for financial support from the National Natural Science Foundation of China (52005108, 52275096), Fuzhou-Xiamen-Quanzhou National Independent Innovation Demonstration Zone High-end Equipment Vibration and Noise Detection and Fault Diagnosis Collaborative Innovation Platform Project, Fujian Provincial Major Research Project (Grant No. 2022HZ024005), as well as the Start-up Funding from Fuzhou University (GXRC-20066). We also thank the technical staff and aegis of the Fuzhou University International Joint Laboratory of Precision Instruments and Intelligent Measurement & Control. The insightful suggestions and comments of three anonymous referees were gratefully received and implemented.

References

[1] Hull D, Clyne TW. An introduction to composite materials. Cambridge, UK: Cambridge University Press; 1996.

[2] Wang B, Seffen KA, Guest SD, Lee T-L, Huang S, Luo S, et al. In-situ multiscale shear failure of a bistable composite tape-spring. Compos Sci Technol 2020;200:108348.

[3] Zhang X, Nie R, Chen Y, He B. Deployable Structures: Structural Design and Static/Dynamic Analysis. J Elast 2021;146:199–235.

[4] Emam SA, Inman DJ. A Review on Bistable Composite Laminates for Morphing and Energy Harvesting. Appl Mech Rev 2015;67:60803–15.

[5] Chi Y, Li Y, Zhao Y, Hong Y, Tang Y, Yin J. Bistable and Multistable Actuators for Soft Robots: Structures, Materials, and Functionalities. Adv Mater 2022:2110384.

[6] Cao Y, Derakhshani M, Fang Y, Huang G, Cao C. Bistable Structures for Advanced Functional Systems. Adv Funct Mater 2021;n/a:2106231.
[7] Yang C, Wang B, Zhong S, Zhao C, Liang W. On tailoring deployable mechanism of a bistable composite tape-spring structure. Compos Commun 2022;32:101171.
[8] Hyer MW. Some Observations on the Cured Shape of Thin Unsymmetric Laminates. J Compos Mater 1981;15:175–94.
[9] Schultz MR. A concept for airfoil-like active bistable twisting structures. J Intell Mater Syst Struct 2008;19:157–69.
[10] Lee AJ, Moosavian A, Inman DJ. A piezoelectrically generated bistable laminate for morphing. Mater Lett 2017;190:123–6.
[11] Daynes S, Potter KD, Weaver PM. Bistable prestressed buckled laminates. Compos Sci Technol 2008;68:3431–7.
[12] Daynes S, Diaconu CG, Potter KD, Weaver PM. Bistable prestressed symmetric laminates. J Compos Mater 2010;44:1119–37.
[13] Wang B, Fancey KS. A bistable morphing composite using viscoelastically generated prestress. Mater Lett 2015;158:108–10.
[14] Wang B, Ge C, Fancey KS. Snap-through behaviour of a bistable structure based on viscoelastically generated prestress. Compos Part B Eng 2017;114:23–33.
[15] Wang J, Nartey MA, Scarpa F, Cui W, Peng H-X. Design and manufacturing of highly tailorable pre-bent bi-stable composites. Compos Struct 2021;276:114519.
[16] Daton-Lovett A. An extendible member. GB9606200A, 1996.
[17] Guest SD, Pellegrino S. Analytical models for bistable cylindrical shells. Proc R Soc A Math Phys Eng Sci 2006;462:839–54.
[18] Seffen KA, Wang B, Guest SD. Folded orthotropic tape-springs. J Mech Phys Solids 2019;123:138–48.
[19] Wang B, Seffen KA, Guest SD. Folded strains of a bistable composite tape-spring. Int J Solids Struct 2021;233:111221.
[20] Chamberlain MK, Kiefer SH, LaPointe M, LaCorte P. On-orbit flight testing of the Roll-Out Solar Array. Acta Astronaut 2021;179:407–14.
[21] Daly RT, Ernst CM, Barnouin OS, Chabot NL, Rivkin AS, Cheng AF, et al. Successful kinetic impact into an asteroid for planetary defense. Nature 2023:1–48.
[22] Lachenal X, Weaver PM, Daynes S. Multi-stable composite twisting structure for morphing applications. Proc R Soc A Math Phys Eng Sci 2012;468:1230–51.
[23] Lachenal X, Daynes S, Weaver PM. A non-linear stiffness composite twisting I-beam, J. Intell. Mater. Syst. Struct. 2013;25:744–54.
[24] Lachenal X, Weaver PM, Daynes S. Influence of transverse curvature on the stability of pre-stressed helical structures. Int J Solids Struct 2014;51:2479–90.
[25] Carey S, Telford R, Oliveri V, McHale C, Weaver P. Bistable composite helices with thermal effects. Proc R Soc A Math Phys Eng Sci 2019;475:20190295.
[26] McHale C, Hadjiloizi DA, Telford R, Weaver PM. Morphing composite cylindrical lattices: enhanced modelling and experiments, J. Mech. Phys. Solid. 2020;135:103779.
[27] Aza C, Pirrera A, Schenk M. Multistable morphing eechanisms of nonlinear springs. J Mech Robot 2019;11:051014.